

Determination of Dopamine in the Presence of Ascorbic Acid on Digitonin-Doped Coal Tar Pitch Carbonaceous Electrode

İlknur Üstündağ* and Aslı Erkal¹

Dumlupınar University, Faculty of Arts & Science, Department of Physics, 43100 Kütahya, Turkey

¹Dumlupınar University, Faculty of Arts & Science, Department of Chemistry, 43100 Kütahya, Turkey

(Received June 10, 2016; accepted September 1, 2016)

Keywords: digitonin, coal tar pitch, carbonaceous electrode, dopamine, differential pulse voltammetry

A novel carbonaceous material was prepared from a digitonin (DG)-doped coal tar pitch (CTP) with a tube furnace under nitrogen atmosphere. It was used as an electrode after mixing the material with an organic binder (resin). The new carbon electrode was denoted as CTP-DG. CTP-DG was characterized by cyclic voltammetry (CV), infrared spectroscopy (IR), X-ray photoelectron spectroscopy (XPS), scanning electron microscopy (SEM), and X-ray diffraction (XRD). The electrode was used for the determination of dopamine (DA) by differential pulse voltammetry (DPV). It exhibits a linear response to DA in the range of 1–60 μM . The detection limit ($S/N = 3$) for DA is 80 nM. Satisfactory results were achieved for the determination of DA in human urine samples.

1. Introduction

Recently, carbonaceous materials (CMs) and their hybrids have been actively pursued as electrocatalysts for electrochemical studies.⁽¹⁾ CMs such as glassy carbon (GC),⁽²⁾ vitreous carbon,⁽³⁾ pyrolyzed photoresist film (ppf)-coated substrates,⁽⁴⁾ carbon nanotubes,⁽⁵⁾ and graphene⁽⁶⁾ are very conductive surfaces as working electrodes. Currently, CMs with natural carbon matrices including products such as plant⁽⁷⁾ and animal⁽⁸⁾ sources are used as next-generation electrodes. In addition, some chemicals such as polysaccharides/osazones,⁽⁹⁾ and polymers⁽¹⁰⁾ are preferred as raw materials. In a previous study,⁽¹¹⁾ an electrode material was synthesized from a prawn shell with enriched chitin under pyrolysis temperature. The material was used as an electrocatalyst for oxygen reduction reaction. In another study,⁽¹²⁾ carbonaceous foam was prepared for biofuel cells. Its electrochemical activity was determined using the catalytic current of a porous electrode that was 13-fold greater than that of a bare GC electrode. Lv *et al.* studied the carbonization of peanut shells.⁽¹³⁾ The untreated and pretreated shells were pyrolyzed using a tubular furnace at 600 °C. The carbonized materials were used as ultralong cycling anodes for lithium and sodium batteries.

Many researchers are still using conventional electrodes such as GC, carbon paste, gold, and platinum. CMs such as a coal tar pitch (CTP) and a CTP composite are not yet commonly used as electrode materials. They are quite an original research topic in electrochemistry and may be used, for example, as sensor templates,⁽¹⁴⁾ electronic device elements,⁽¹⁵⁾ heat exchangers,⁽¹⁶⁾ and supercapacitors.⁽¹⁷⁾ The CTP is a very low cost material⁽¹⁸⁾ for these studies and an excellent precursor for carbonaceous composites.⁽¹⁹⁾ It has high conductivity and stability, and a large surface

*Corresponding author: e-mail: iozkirim@gmail.com
<http://dx.doi.org/10.18494/SAM.2017.1416>

area.⁽²⁰⁾

The dopamine (DA) molecule is vital for the central and peripheral nervous systems.⁽²¹⁾ The determination of the DA molecule has great significance. DA, ascorbic acid (AA), and uric acid (UA) usually coexist in food and biological samples.⁽²²⁾ Thus, the determination of DA in the presence of AA is very significant.

In this study, digitonin (DG), which is a kind of glycoside, was added into a CTP. The carbonized product was denoted as CTP-DG. The material was carbonized with a tube furnace at 1000 °C under inert N₂ flow at a heating rate of 10 °C/min for a hold period of 1 h. The carbonized solid was ground into fine powder in a planetary ball mill. The material was characterized by some techniques such as electrochemical, spectroscopic, and microscopic methods. It was used as an electrode material after mixing it with a resin as an organic binder. The electrode was used in the determination of DA by differential pulse voltammetry (DPV). The developed method was used for the determination of DA in real samples.

2. Experimental Procedure

All chemicals were of reagent grade and used without further purification. They were obtained from commercial suppliers such as Merck, Fluka, Sigma-Aldrich, and Riedel. The CTP was purchased from Orcan Asfalt ve Yalitim Urunleri Company (Tuzla-Istanbul, Turkey). Bare GC working electrodes were obtained from GC-20 (Tokai, Japan). CTP-DG, CTP, and GC electrodes were cleaned and polished on a microped (Buehler, Lake Bluff, IL, USA) with 100 and 50 nm aluminum oxide suspensions (Baikowski, USA). Then, the polished carbon electrodes were sonicated with an ultrasonic bath (SK1200H ultrasonic cleaner, China) in ultrapure water (UPW, 18.2 MΩ cm, Human Power 1+, South Korea) and in 1:1 (v/v) isopropyl alcohol (IPA)/acetonitrile (MeCN) solutions for approximately 7 min. Electrochemical measurements were performed using an Ivium CompactStat, (U.S.) electroanalyzer. All data were acquired with a triple-electrode system at room temperature (25 ± 1 °C) under a high-purity argon (99.999%) atmosphere. A platinum wire was used as an auxiliary electrode. Ag/AgCl/KCl_(sat) and Ag/AgNO₃ (0.01 M) were used as reference electrodes for aqueous and nonaqueous media, respectively.

2.1 Synthesis of carbonized CTP-DG

CTP-DG was prepared with a DG-doped CTP. The amount of DG in the CTP was adjusted as 1% (w/w). 10 g of the DG-added CTP composite was carbonized in a N₂-atmosphere tube furnace (Protherm, Turkey) with a heating rate of 10 °C/min to reach 1000 °C. This was followed by the annealing of the materials at 1000 °C in N₂ atmosphere for 1 h. The black material transformed into metallic grey. The carbonized solid (CTP-DG) was ground into fine powder in a planetary ball mill PM100 (Retsch, Germany). In addition, a pure CTP electrode was synthesized under the same conditions for comparison with the CTP-DG electrode.

A very small amount of “kamalak” resin (*Cedrus libani* A. Rich.) was sprayed in 2 g of CTP and CTP-DG powder. The moistened powders were pressed into pellets of 10 mm diameter. The disc pellets were dried with an oven at 55 °C under vacuum. The electrodes were packed into the cavity of a politetrafluoroetilen (Teflon) tube. The electrode surface area is 0.073 cm² in the Teflon tube. Parts of the CTP-DG working electrode and cell system are shown in Fig. 1.

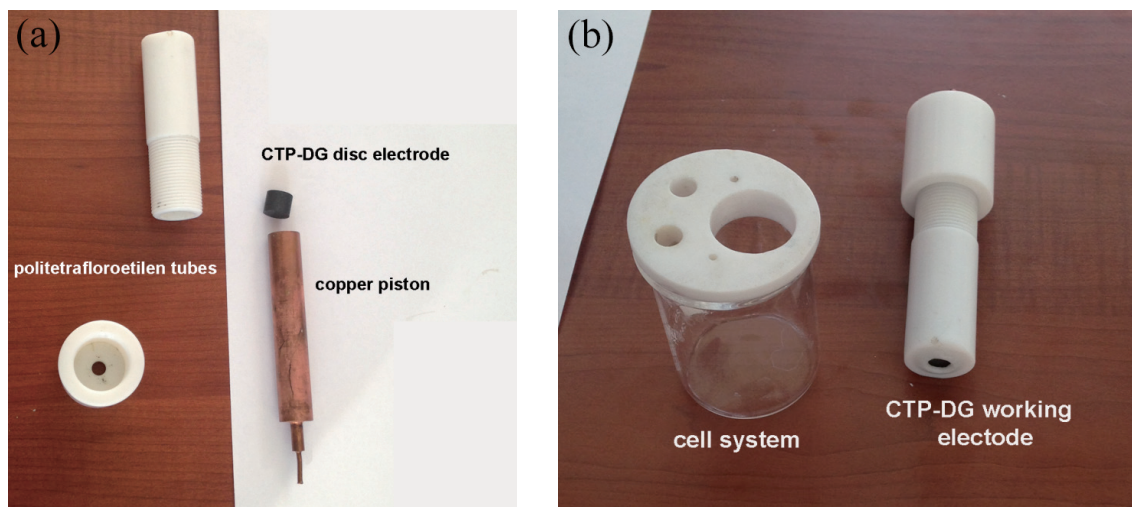


Fig. 1. (Color online) Parts of (a) CTP-DG working electrode and (b) cell system.

2.2 Characterization of CM

The CMs were characterized with ferrocene and ferricyanide/ferrocyanide redox probes by cyclic voltammetry (CV) and EIS techniques, respectively. All three electrodes (GC, CTP, and CTP-DG) were placed in the Teflon tube. Electrochemical results of the CTP-DG electrode were compared with those of the CTP and GC electrodes. The stability of the CTP-DG electrode was tested with ferrocene by CV when it was kept in an open atmosphere for 10 d.

The infrared spectroscopy (IR) measurement of the CTP and CTP-DG electrodes was performed in a Bruker Tensor 27 (Germany) FT-IR spectrophotometer with a diamond-ATR accessory (Harrick Scientific, USA). X-ray diffraction (XRD) measurements of the CTP and CTP-DG electrodes were obtained with a Rigaku Miniflex (Japan) X-ray diffractometer. Scanning electron microscopy (SEM) images were obtained using a SEM system (Zeiss-Evo, Germany). X-ray photoelectron spectroscopy (XPS) data was obtained with an X-ray photoelectron spectrometer [PHI 5000, Versa Probe [Φ ULVAC-PHI, Inc., Japan/USA) with monochrome Al K α radiation (1486.6 eV) as an X-ray anode and operated with 50 W at 10^{-7} Pa.

2.3 Calibration study of DA in aqueous media

The electrocatalytic activities of the GC, CTP, and CTP-DG electrodes were determined via DPV. A comparison of DPVs of DA on all electrodes was carried out. CV studies of DA at various scan rates (10 to 300 mV/s) were performed in 0.1 M PBS ($pH = 7$). Various concentrations (1 to 60 μ M) of DA standards in the presence of 5 mM AA were spiked into the cell. DPV results were recorded by positive scanning at a rate of 20 mV s $^{-1}$, a pulse amplitude of 25 mV, a pulse rate of 0.5 s, and a pulse width of 60 ms for a holding time of 2 s. Calibration curves of DA were plotted at 25 ± 1 °C. The limits of detection (LODs) of the developed method were calculated ($S/N = 3$).

2.4 Sample analysis

The CTP-DG electrode was applied to the determination of DA in human urine samples. A 100 μL urine sample without any sample pretreatment was directly added into the electrolyte solution and analyzed by DPV. All measurements were repeated three times.

3. Results and Discussion

3.1 Characterization of CTP-DG

Cyclic voltammograms of 2 mM ferrocene redox probes in 0.1 M TBATFB in MeCN on the GC, CTP, and CTP-DG electrodes are given in Fig. 2(a). The electron transfer rate of the redox probe is partially higher on the CTP-DG surface than on the CTP and GC surfaces [Fig. 2(a)]. The anodic peak currents of the redox probes on the GC, CTP, and CTP-DG electrodes were calculated as 39.2 ± 2.3 , 50.3 ± 2.7 , and 87.1 ± 1.2 μA , respectively. The electrode stability of CTP-DG was tested with ferrocene by CV [Fig. 2(b)]. The electrode was kept in an open atmosphere for 10 d. The anodic peak current of the CTP-DG electrode did not change even after 10 d.

The electrode performance characteristics of the GC, CTP, and CTP-DG electrodes were investigated by EIS using a 2 mM $\text{K}_3\text{Fe}(\text{CN})_6/\text{K}_4\text{Fe}(\text{CN})_6$ redox probe in 0.1 M KCl media. The Nyquist plots of all the three electrodes are shown in Fig. 3. All Nyquist plots were fitted with a diffusion-controlled CPE equivalent electrical circuit.⁽²³⁾ The charge transfer resistance (R_{ct}) of redox probes was decreased using the CTP-DG electrode as in the cases of the GC and CTP electrodes. The electron transfer of the redox couple was accelerated on the CTP-DG electrode. The R_{ct} values of the CTP-DG, GC, and CTP electrodes were fitted as 4.2, 6.4, and 5.7 $\text{k}\Omega$,

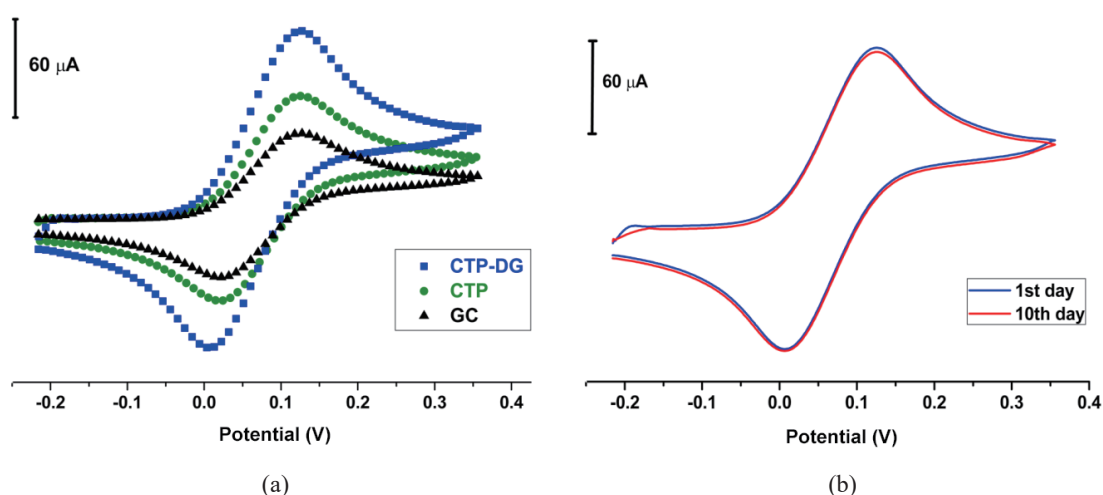


Fig. 2. (Color online) (a) Cyclic voltammograms of 2 mM ferrocene on GC, CTP, and CTP-DG electrodes in 0.1 M TBATFB in MeCN with a scan rate of 200 mVs^{-1} vs $\text{Ag}/\text{Ag}^+(0.1 \text{ M})$. (b) Cyclic voltammogram of ferrocene on the CTP-DG electrode when it is kept in an open atmosphere for 10 d.

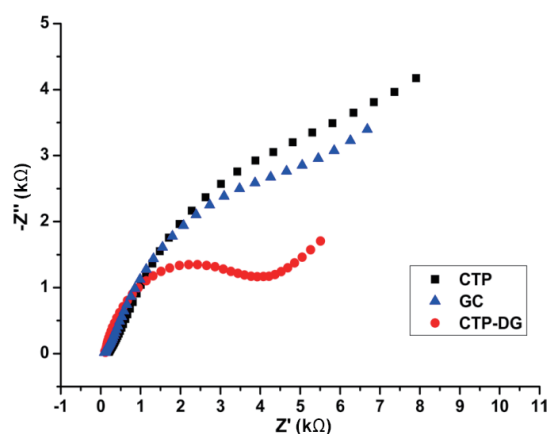


Fig. 3. (Color online) Nyquist plots of 2 mM $\text{K}_3\text{Fe}(\text{CN})_6/\text{K}_4\text{Fe}(\text{CN})_6$ in 0.1 M KCl on the CTP-DG, GC, and CTP electrodes vs Ag/AgCl/KCl sat. Frequency ranges from 100 kHz to 0.2 Hz with 10 mV wave amplitude at a DC potential of 75 mV for redox couple.

respectively.

IR measurements were carried out in the wavenumber range of 400–4000 cm^{-1} . FT-IR spectra of the CTP-DG, DG, and CTP electrodes are given in Fig. 4(a). The bands at 3350 and 1050 cm^{-1} in the IR spectrum of the DG electrode are assigned to the stretching vibrations of OH and C–O, respectively. The material has two bands between 3010 and 2790 cm^{-1} and 1500 and 1350 cm^{-1} for aliphatic C–H stretching and bending, respectively.⁽²⁴⁾ IR spectra of CTP and CTP-DG are similar. Both materials contain a carbon skeleton. The π -bonded C–H (in alkene and aromatic ring) and aliphatic C–H stretching vibrations appear between 3140 and 2790 cm^{-1} . The band of the aliphatic C–H stretching of the DG-doped CTP is more intense than the stretching peak of the CTP due to DG, which is only an aliphatic compound. Similarly, the band of the π -bonded C–H stretching of the CTP is more intense than the stretching peak of CTP-DG. C–H deformation bands are observed between 650 and 1030 cm^{-1} . The aromatic ring modes of both electrodes are observed between 1400 and 1615 cm^{-1} .^(25,26)

XPS measurements were carried out on CTP-DG. High-resolution XPS scan for C1s is given in Fig. 4(b). The C1s spectrum was curve-fitted as sp^2 - and sp^3 -hybridized carbons at 284.5 and 286.0 eV, respectively.^(27,28) This technique showed that the material includes aliphatic and aromatic/alkene groups.

XRD patterns of the CTP and CTP-DG are given in Fig. 5. Both materials have two main peaks at 25.3 and 43.1°. The patterns are assigned to the (002) and (100) sequences for carbon atoms.⁽²⁹⁾ This shows that both materials have a regular form via a thermal process. The pattern of the CTP is sharper than that of CTP-DG. The signal intensity of the glycoside-doped CTP has declined slightly owing to the crystalline form.

SEM images of the CTP and CTP-DG are given in Figs. 6(a) and 6(b), respectively. SEM images were taken from powder form of the solids after a thermal process. The image of the CTP was obtained from a foil-flake form. The image of the CTP shows a regular structure, such as graphene. In Fig. 6(b), the cavities of flakes were filled with DG. The structure of the DG-doped CTP is much more regular than that of the CTP.

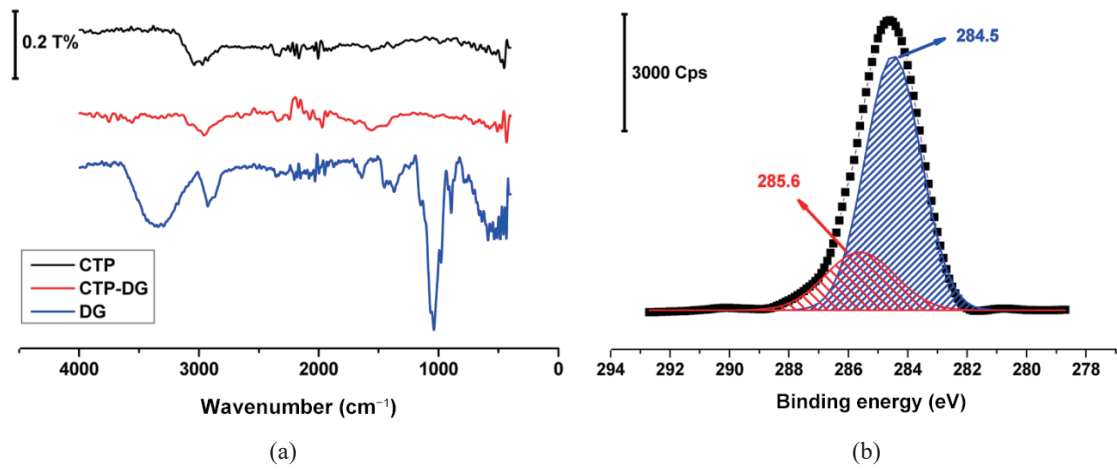


Fig. 4. (Color online) (a) IR spectra of the CTP-DG and CTP and (b) XPS spectrum of the CTP-DG: high-resolution scans for C1s.

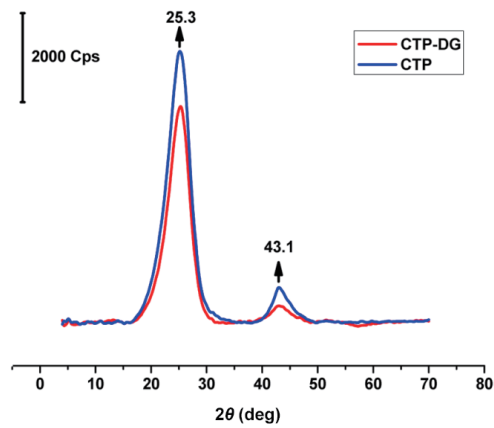


Fig. 5. (Color online) XRD patterns of CTP and CTP-DG.

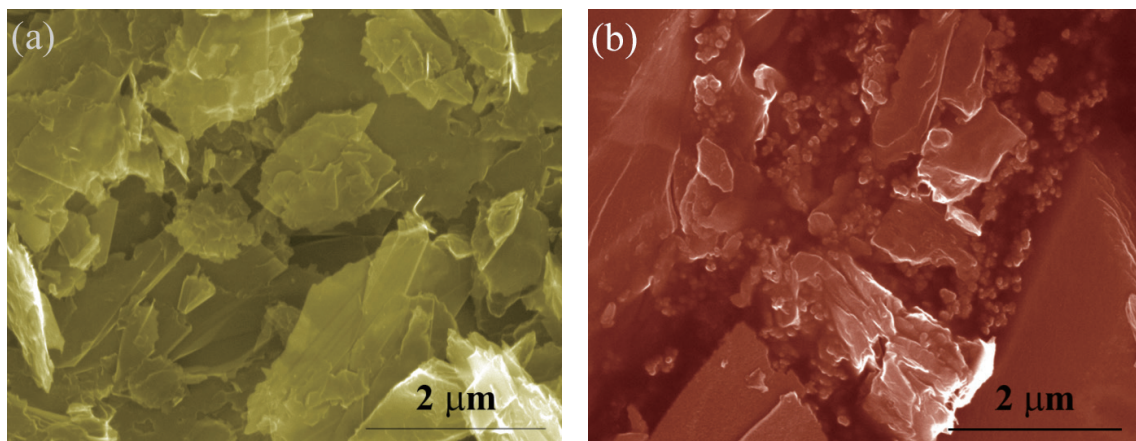


Fig. 6. (Color online) SEM images of (a) CTP and (b) CTP-DG.

3.2 Calibration study of DA in the presence of AA

Differential pulse voltammograms of DA on the GC, CTP, and CTP-DG electrodes are given in Fig. 7(a). The highest oxidation peak current value was obtained on the CTP-DG. The DPV response of DA on CTP-DG supported the response of the $K_3Fe(CN)_6/K_4Fe(CN)_6$ redox probe on the same electrode. The peak current of 60 μM DA on GC, CTP, and CTP-DG was calculated as 9.1, 23.3, and 111.2 μA , respectively. The CTP-DG has the highly electrocatalytic effect for DA.

Cyclic voltammograms at various scan rates (10–300 mV/s) for 0.2 mM DA at the CTP-DG disc electrode are given in Fig. 7(b). CV results showed that the oxidation peak current of DA increased with the scan rate. As shown in Fig. 7, the oxidation peak current was proportional to the square root of the scan rate. The oxidation of DA seemed to be a diffusion-controlled process with I_p (μA) = $6.0023[v]^{1/2} - 17.075$ ($R^2 = 0.9899$).

DPV measurements were performed for DA in the presence of 5 mM AA in PBS (pH: 7). The concentration range of DA was 1–60 μM . Figure 8(a) shows the DPV recordings at various concentrations of DA at the CTP-DG disc electrode. The peak potentials of AA and DA were found as -37 and 148 mV, respectively. The linear response to DA in the range of 1 to 60 μM is given in Fig. 8(b). The linear equation for DA was $I_{p(\text{DA})} = 1.7297[\text{DA}] + 4.8984$ ($R^2: 0.9961$) with the linear range of 1 to 60 μM . The LOD is 0.08 μM .

The various LODs obtained with the developed sensor are compared with those of the other reported methods. The results are given in Table 1. The developed electrode could provide a good platform for the effective electroanalytical detection.

3.3 Precision and accuracy results of the method

Three different DA concentrations (2.0, 5.0, and 7.0 μM) in the linear range were analyzed in five independent series on the intraday and interday. The results are given as data percentages in

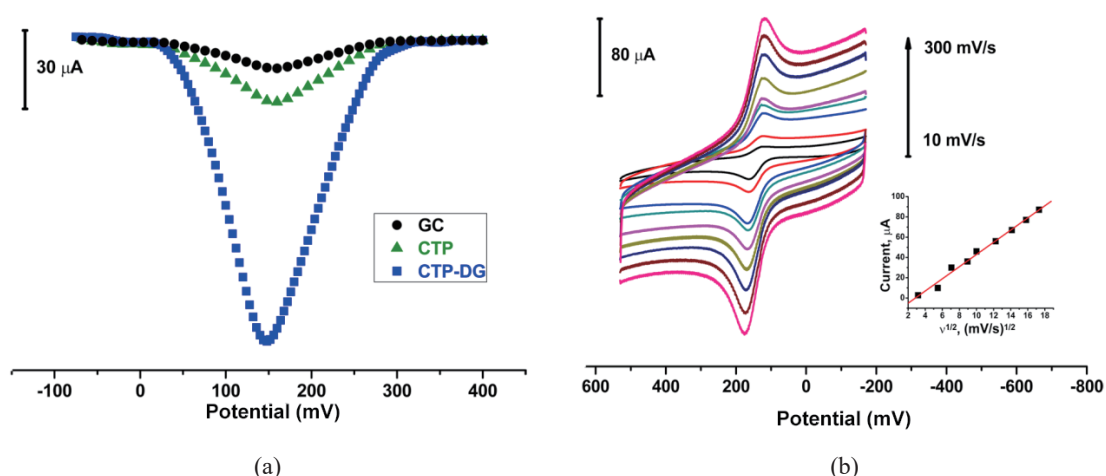


Fig. 7. (Color online) (a) DPVs of 60 μM DA on GC, CTP, and CTP-DG, and (b) CV results of 0.2 mM DA on CTP-DG at various scan rates (10–300 mV/s) in a 0.1 M PBS (pH 7.0) and their linear curve between the current of the oxidation peak and the square root of the scan rate.

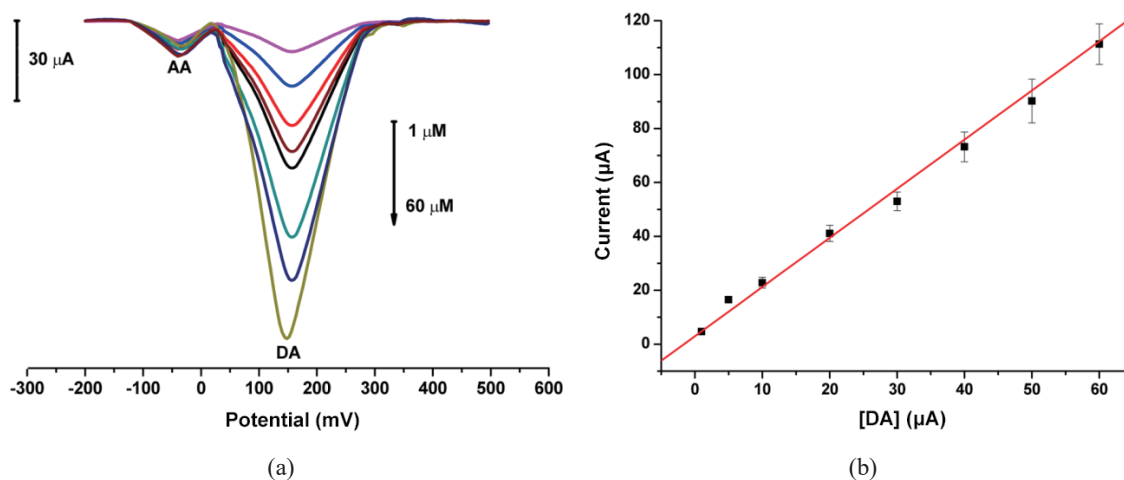


Fig. 8. (Color online) (a) DPVs of 1–60 μM DA on CTP-DG in the presence of AA and (b) their calibration curve.

Table 1
Responses of various voltammetric sensors to DA.

Electrode	Calibration (μM)		Reference
	Range	LOD	
ERGO-FA/GCE	0.6–1000	0.19	30
Graphene	4–100	2.64	31
MWCNT/CCE	0.5–100.0	0.31	32
SPGNE	0.5–2000	0.12	33
AuNCs/AGR/MWCNT/GCE	1.0–210	0.08	34
PtNPs-MWCNT/GCE	0.06–2.03	0.05	35
RGO-AuNPs-CSHMs	1.0–200	0.3	36
CILE	2.0–1500	1.0	37
s-GONR-GCE	0.1–8.5	0.024	38
PIn5COOH	0.5–20	0.1	39
CTP-DG	1–60	0.08	This study

ERGO-FA/GCE: electrochemically reduced graphene oxide-ferulic acid, MWCNT/CCE: multiwall carbon-nanotube-modified carbon-ceramic electrode, SPGNE: screen-printed graphene electrode, AuNCs/AGR/MWCNT: gold nanoclusters/activated graphene multiwall carbon-nanotube nanocomposite, PtNPs-MWCNT/GCE: Pt nanoparticles decorating multiwall carbon-nanotube-modified glassy carbon electrode, RGO-AuNPs-CSHMs: reduced graphene oxide and Au nanoparticles entrapped in chitosan/silica sol-gel hybrid membranes, CILE: carbon ionic liquid electrode, s-GONR-GCE: short graphene oxide-nanoribbon-modified GC electrode, and PIn5COOH: poly(indole-5-carboxylic acid) electrode.

Table 2
Precision and accuracy results of the method.

Found Value, precision % (RSD), and accuracy %	Added (DA)			
	2 μM	5 μM	7 μM	
Intraday*	Found Value	2.01 ± 0.02	5.04 ± 0.03	7.06 ± 0.05
	RSD %	1.00	0.60	0.71
	Accuracy %	0.50	0.80	0.86
Interday*	Found Value	2.00 ± 0.03	4.98 ± 0.02	7.11 ± 0.06
	RSD %	1.50	0.40	0.84
	Accuracy %	0	-0.40	1.57

*Five independent series on the same day for intraday precision and five consecutive days for interday precision from five measurements of every series.

Table 3
Effects of some groups on the peak currents of 1 μM DA in 0.1 M PBS (pH 7.0).

Interferences	Concentration (μM)	Signal change of DA
		DA
Na^+	1000	-3.67%
K^+	1000	-2.01%
NH_4^+	1000	2.03%
Mg^{2+}	1000	-1.27%
Zn^{2+}	1000	2.46%
Cl^-	1000	-2.28%
NO_3^-	1000	-0.20%
SO_4^{2-}	1000	4.43%
Uric acid	200	-0.55%
Folic acid	200	0.47%
D-glucose	1000	0.21%
L-alanine	1000	0.97%
Aspartic acid	1000	0.55%

Table 4
Analytical recovery of DA from urine samples ($N = 5$).

Sample	Added DA (μM)	Detected by DPV (μM)	Recovery (%)
Urine I	–	–	–
	5	4.98	99.6
	10	10.07	100.7
Urine II	20	20.71	103.6
	–	–	–
	5	5.12	102.4
Urine III	10	9.88	98.8
	20	20.04	100.2
	–	–	–
Urine III	5	5.02	100.2
	10	10.33	103.3
	20	19.81	99.05

Table 2. The precision values (RSD %) varied from 0.60 to 1.00 for intraday precision and from 0.40 to 1.50 for interday precision. The accuracy of the developed method was calculated as the percent of relative error. The accuracy values (%) varied from 0.50 to 0.86 for intraday precision and from 0 to 1.57 for interday precision. Results were calculated within the acceptable limits.

3.4 Interference

The effects of some important biological substances and ions on the peak currents of 1 μM DA in 0.1 M PBS (pH 7.0) are given in Table 3. Current signal changes are approximately ≤ 4.43 and $\geq -3.67\%$. Therefore, in the interference study, the interference effect of these groups in the selected concentration range is not an important factor.

3.5 Determination of DA in human urine samples

We determined DA in three human urine samples using the standard addition method to evaluate the validity and reliability of the proposed method. The samples were diluted 50 times using PBS (0.1 M, pH 7.0). DPV results were recorded after 200 μL of urine sample was added into 10 mL of the buffer solution. The measurements are presented in Table 4. The recovery of the samples ranged between 98.8 and 103.6%. The results showed the successful application of the CTP-DG carbonaceous electrode to the determination of DA in urine samples.

4. Conclusions

A carbonized CTP-DG disc electrode was prepared with the pyrolysis of a DG-CTP mixture. The electrode materials were characterized by CV, EIS, XPS, IR, XRD, and SEM. The electrode was pressed into thick pellets. This electrode was used for the determination of DA in the presence of AA via DPV. The electron transfer rate of DA significantly increased via the electrocatalytic

effect on the CTP-DG electrode. The linear equation for DA was $I_{p(DA)} = 1.7297[DA] + 4.8984$ ($R^2: 0.9961$) with the linear range of 1 to 60 μM in the presence of 5 mM AA. The LOD ($S/N = 3$) of the developed method was 0.08 μM . Accuracy and precision were calculated within acceptable limits. The developed method was applied to human urine samples. The maximum analytical recovery of DA via the method added to urine samples was calculated as $\leq 103.6\%$.

References

- 1 J. C.-García and C. R. Cabrera: *Electrocatalysis* **5** (2014) 402.
- 2 S. Majidi, A. Jabbari, H. Heli, H. Yadegari, A. A. Moosavi-Movahedi, and S. Haghgoo: *J. Solid State Electrochem.* **13** (2009) 407.
- 3 V. E. Norvell and G. Mamantov: *Anal. Chem.* **49** (1977) 1470.
- 4 A. J. Gross and A. J. Downard: *Anal. Chem.* **83** (2011) 2397.
- 5 Y. Wen, J.-S. Ye, W.-D. Zhang, F.-S. Sheu, and G. Q. Xu: *Microchim. Acta* **162** (2008) 235.
- 6 A. B. M. Zakaria, E. S. Vasquez, K. B. Walters, and D. Leszczynska: *RSC Adv.* **5** (2015) 107123.
- 7 Y. Gao, L. Li, Y. Jin, Y. Wang, C. Yuan, Y. Wei, G. Chen, J. Ge, and H. Lu: *Appl. Energy* **153** (2015) 41.
- 8 V. Selvamani, R. Ravikumar, V. Suryanarayanan, D. Velayutham, and S. Gopukumar: *Electrochim. Acta* **182** (2015) 1.
- 9 Y. Fan, P.-F. Liu, Z.-J. Yang, T.-W. Jiang, K.-L. Yao, R. Han, X.-X. Huo, and Y.-Y. Xiong: *Electrochim. Acta* **163** (2015) 140.
- 10 Z. Wang, S. Zhang, L. Zhang, R. Lin, X. Wu, H. Fang, and Y. Ren: *J. Power Sources* **248** (2014) 337.
- 11 Y. Li, H. Zhang, P. Liu, Y. Wang, H. Yang, Y. Li, and H. Zhao: *Electrochem. Commun.* **51** (2015) 6.
- 12 V. Flexer, N. Brun, R. Backov, and N. Mano: *Energy Environ. Sci.* **3** (2010) 1302.
- 13 W. Lv, F. Wen, J. Xiang, J. Zhao, L. Li, L. Wang, Z. Liu, and Y. Tian: *Electrochim. Acta* **176** (2015) 533.
- 14 F. Montilla, E. Morallón, J. L. Vázquez, J. A.-Monge, D. C.-Amorós, and A. L.-Solano: *Carbon* **40** (2002) 2193.
- 15 Y.-X. Wang, S.-L. Chou, J. H. Kim, H.-K. Liu, and S.-X. Dou: *Electrochim. Acta* **93** (2013) 213.
- 16 H. Liu, T. Li, X. Wang, W. Zhang, and T. Zhao: *J. Anal. Appl. Pyrolysis* **110** (2014) 442.
- 17 X.-J. He, X.-J. Li, X.-T. Wang, N. Zhao, M.-X. Yu, and M.-B. Wu: *New Carbon Mater.* **29** (2014) 493.
- 18 M. Yamaoka, S.-S. Asami, N. Funaki, S. Kimura, L. Yingjie, T. Fukuda, and M. Yamashita: *PLoS One* **8** (2013) e62903/1.
- 19 C. Blanco, R. Santamaría, J. Bermejo, and R. Menéndez: *Carbon* **38** (2000) 517.
- 20 L. Hao, X. Li, and L. Zhi: *Adv. Mater.* **25** (2013) 3899.
- 21 S. Basu and P. S. Dasgupta: *J. Neuroimmunol.* **102** (2000) 113.
- 22 X. Ouyang, L. Luo, Y. Ding, B. Liu, D. Xu, and A. Huang: *J. Electroanal. Chem.* **748** (2015) 1.
- 23 A. Erkal, M. S. Erdoğan, İ. Aşık, H. Ekşi, S. Jeon, A. O. Solak, and Z. Üstündağ: *J. Electrochem. Soc.* **161** (2014) H696.
- 24 J. A.-Monge and D. C.-Amorós: *Fuel* **80** (2001) 41.
- 25 M. E.-Gemayel, A. Narita, L. F. Dössel, R. S. Sundaram, A. Kiersnowski, W. Pisula, M. R. Hansen, A. C. Ferrari, E. Orgiu, X. Feng, K. Müllen, and P. Samori: *Nanoscale* **6** (2014) 6301.
- 26 Y. I. Kurys, O. O. Ustavytska, V. G. Koshechko, and V. D. Pokhodenko: *Electrocatalysis* **6** (2015) 117.
- 27 S.-K. Jerng, D. S. Yu, J. H. Lee, C. Kim, S. Yoon, and S.-H. Chun: *Nanoscale Res. Lett.* **6** (2011) 565.
- 28 A. Erkal, İ. Üstündağ, S. Yavuz, and Z. Üstündağ: *J. Electrochem. Soc.* **162** (2015) H213.
- 29 Z. Guo, C. Wang, M. Chen, and M. Li: *Int. J. Electrochem. Sci.* **8** (2013) 2702.
- 30 H. S. Han, H. Seol, D. H. Kang, M. S. Ahmed, J.-M. You, and S. Jeon: *Sens. Actuators, B* **204** (2014) 289.
- 31 C. Xiao, X. Chu, Y. Yang, X. Li, X. Zhang, and J. Chen: *Biosens. Bioelectron.* **26** (2011) 2934.
- 32 B. Habibi and M. H. P.-Azar: *Electrochim. Acta* **55** (2010) 5492.
- 33 J. Ping, J. Wu, Y. Wang, and Y. Ying: *Biosens. Bioelectron.* **34** (2012) 70.
- 34 A. A. Abdelwahab and Y.-B. Shim: *Sens. Actuators, B* **221** (2015) 659.
- 35 Z. Dursun and B. Gelmez: *Electroanalysis* **22** (2010) 1106.
- 36 X. Liu, L. Xie, and H. Li: *J. Electroanal. Chem.* **682** (2012) 158.
- 37 A. Safavi, N. Maleki, O. Moradlou, and F. Tajabadi: *Anal. Biochem.* **359** (2006) 224.
- 38 C. L. Sun, C. HaoSu, and J. ZhouWu: *Biosens. Bioelectron.* **67** (2015) 327.
- 39 J. Maciejewska, K. Pisarek, I. Bartosiewicz, P. Kryszynski, K. Jackowska, and A. T. Bieganski: *Electrochim. Acta* **56** (2011) 3700.